Virus specificity and nucleoporin requirements for MX2 activity are affected by GTPase function and capsid-CypA interactions

Bailey Layish[1], Ram Goli[1], Haley Flick[1], Szu-Wei Huang[2], Robert Z. Zhang[1], Mamuka Kvaratskhelia[2], Melissa Kane[1*]

[1]Department of Pediatrics, Division of Infectious Diseases, University of Pittsburgh School of Medicine, Pittsburgh, PA 15224, USA

[2]Division of Infectious Diseases, University of Colorado Anschutz Medical Campus, Aurora, CO 80045, USA

*Address correspondence to Dr. M. Kane, Tel. (412-692-5493); e-mail: kaneme@pitt.edu

Short title: MX2 interactions with CypA and HIV-1

Abstract

Human myxovirus resistance 2 (MX2/MXB) is an interferon-induced GTPase that inhibits human immunodeficiency virus-1 (HIV-1) infection by preventing nuclear import of the viral preintegration complex. The HIV-1 capsid (CA) is the major viral determinant for sensitivity to MX2, and complex interactions between MX2, CA, nucleoporins (Nups), cyclophilin A (CypA), and other cellular proteins influence the outcome of viral infection. To explore the interactions between MX2, the viral CA, and CypA, we utilized a CRISPR-Cas9/AAV approach to generate CypA knock-out cell lines as well as cells that express CypA from its endogenous locus, but with specific point mutations that would abrogate CA binding but should not affect enzymatic activity or cellular function. We found that infection of CypA knock-out and point mutant cell lines with wild-type HIV-1 and CA mutants recapitulated the phenotypes observed upon cyclosporine A (CsA) addition, indicating that effects of CsA treatment are the direct result of blocking CA-CypA interactions and are therefore independent from potential interactions between CypA and MX2 or other cellular proteins. Notably, abrogation of GTP hydrolysis by MX2 conferred enhanced antiviral activity when CA-CypA interactions were abolished, and this effect was not mediated by the CA-binding residues in the GTPase domain, or by phosphorylation of MX2 at position T151. We additionally found that elimination of GTPase activity also altered the Nup requirements for MX2 activity. Our data demonstrate that the antiviral activity of MX2 is affected by CypA-CA interactions in a virus-specific and GTPase activity-dependent manner. These findings further highlight the importance of the GTPase domain of MX2 in regulation of substrate specificity and interaction with nucleocytoplasmic trafficking pathways.

Author Summary

HIV-1 entry into the nucleus is an essential step in viral replication that involves complex interactions between the viral capsid and multiple cellular proteins, including the proline isomerase cyclophilin A. Nuclear entry of HIV-1 and other primate lentiviruses is inhibited by the antiviral protein MX2. Here, we show that direct interactions between capsid and cyclophilin A

28 affect the antiviral activity and specificity of MX2, and that these interactions are altered when the
29 enzymatic activity of MX2 is eliminated. We demonstrate that abolishing enzymatic activity of MX2
30 also alters the requirements for nuclear pore complex components for viral restriction. Our study
31 provides new insights into how the enzymatic function of MX2 affects inhibition of lentiviral nuclear
32 import.
33

34 **Introduction**

35 Innate immune detection of viral infection results in the production of type I interferons (IFNs),
36 which in turn induce the expression of hundreds of IFN-stimulated genes (ISGs) that confer an
37 'antiviral' state, impeding the propagation of many viruses (1, 2). Among the antiviral ISGs are
38 the dynamin-like guanosine triphosphatases (GTPases) *MX1* (*MXA*) and *MX2* (*MXB*). Both
39 proteins contain an amino-terminal GTPase domain connected to a carboxy-terminal stalk domain
40 via a tripartite bundle signaling element (BSE) (3). MX1 is exclusively found in the cytoplasm,
41 while MX2 contains a nuclear localization signal (NLS)-like sequence in its first 25 amino acids
42 and localizes at the nuclear pore complex (NPC) (4-6). MX1 has long been known as a broadly
43 acting and potent antiviral protein (3), while MX2 was ascribed with antiviral function in 2013 as
44 an inhibitor of HIV-1 and other primate lentiviruses, and later shown to also restrict replication of
45 herpesviruses and hepatitis B and C viruses (6-11).

46 MX2 inhibits HIV-1 infection prior to the chromosomal integration of proviral DNA, but after
47 the completion of reverse transcription (6, 7, 12), and current models suggest that it acts by
48 preventing nuclear import of the viral preintegration complex. The viral capsid (CA) is the major
49 viral determinant of MX2 sensitivity, and several single amino-acid substitutions in CA have been
50 identified that confer partial or complete resistance to MX2 (6-8, 13, 14). MX2 has also been found
51 to directly bind the HIV-1 CA, however the relevance of this binding for viral inhibition is unclear
52 since MX2-resistant CA proteins are still efficiently bound by MX2 (15, 16).

53 The antiviral activity of MX1 has been extensively investigated, and current understanding
54 indicates that engagement of MX1 with components of viral replication complexes (such as the

55 nucleoprotein of orthomyxoviruses) results in higher order oligomerization, followed by GTP
56 hydrolysis and conformational changes which lead to the perturbation of viral
57 transcription/replication via mislocalization of targeted components, blocking nuclear
58 translocation, and/or disruption of the functional integrity of the replication complex. GTPase
59 function and higher order oligomerization are generally required for antiviral activity of MX1 (3).
60 Conversely, GTP binding and hydrolysis are dispensable for the antiviral activity of MX2 (6, 7,
61 17), and although dimerization is essential, higher order oligomerization is not required for viral
62 restriction (16, 18). Finally, while anti-viral specificity of MX1 is largely determined by a disordered
63 loop (L4) in the stalk domain (19), antiviral specificity of MX2 is determined by the N-terminal
64 domain (NTD) (13, 17), indicating that the mechanisms underlying inhibition of viral infection by
65 MX1 and MX2 are distinct. The antiviral activity of MX2 is also regulated by protein
66 phosphorylation. Phosphorylation of serines 14, 17, and 18 in the NTD suppresses antiviral
67 activity and alters interactions with the viral CA and accumulation at the nuclear envelope, while
68 dephosphorylation by myosin light chain phosphatase (MLCP) upon IFN stimulation restores
69 antiviral function (20). Phosphorylation status of additional residues throughout all domains of
70 MX2 also alter the antiviral activity and specificity of MX2 (21). Thus, a variety of determinants
71 throughout MX2 modulate its function and viral specificity.

72 Sensitivity of HIV-1 to MX2 activity is affected by complex interactions between CA and
73 cellular proteins involved in the early stages of HIV-1 infection, including nucleoporins (Nups) and
74 the peptidyl-prolyl isomerase cyclophilin A (CypA) (reviewed in (22)). CypA-CA interactions can
75 affect many early steps of HIV-1 replication, disruption of the interaction between HIV-1 and CypA,
76 either genetically or by cyclosporine A (CsA) addition, reduces the efficiency of HIV-1 infection
77 (reviewed in (23)), and some studies have indicated that CypA-CA interactions influence nuclear
78 entry (24, 25), and more recently CypA has been shown to protect the HIV-1 CA from restriction
79 by TRIM5α (26, 27). However, it remains unclear whether the isomerase activity of CypA plays a
80 role in its pro-viral function, since mutations that abolish enzymatic activity also affect CA-binding.
81 Indeed, defining a precise role for CypA in HIV-1 infection has proved difficult because CsA

82 treatment has diverse enhancing and inhibiting effects on infection that are determined by CA
83 mutations and target cell type, suggesting that the function of CypA in HIV-1 infection is
84 differentially affected by other cellular proteins in various contexts (reviewed in (23, 28)).

85 Here, we investigated the effects of CA-CypA interactions on the antiviral activity and
86 specificity of MX2. We find that the effects of CypA on MX2 activity against HIV-1 are the direct
87 result of CA-CypA interactions. We also identified cell-type-dependent determinants for the
88 GTPase and oligomerization requirements for MX2 activity. We show that abrogation of GTP
89 hydrolysis by MX2 conferred enhanced antiviral activity when CA-CypA interactions were
90 abolished. This activity is independent of previously reported CA-binding residues in the GTPase-
91 domain of MX2. Finally, we show that GTPase-deficient MX2 has altered nucleoporin
92 requirements for antiviral activity. These results indicate that GTPase function alters substrate
93 specificity and antiviral function of MX2.

94

95 **Results**

96 **The effects of CypA on MX2 activity are mediated by direct interactions between CypA and**
97 **the viral CA.** Multiple previous reports have demonstrated that CsA addition abolishes the
98 antiviral activity of MX2 against wild-type HIV-1 (HIV-1_{WT}) (8, 29, 30), and CA mutants unable to
99 bind CypA (eg. G89V and P90A) are MX2-resistant (6-8, 12, 14, 15, 30) suggesting that MX2 is
100 only active against CypA bound HIV-1. However, CA mutations have multiple pleiotropic effects,
101 and CsA treatment targets multiple cyclophilin proteins (23, 31, 32). Furthermore, CypA also has
102 multiple cellular functions that affect protein folding, trafficking, interaction, and activation (33).
103 Therefore, to address whether there are capsid-independent effects of CypA on HIV-1 infection
104 or MX2 activity, we generated CypA knock-out cell lines as well as cells expressing CypA from its
105 endogenous locus but with specific point mutations introduced to alter CA-binding specificity.
106 TRIMCyp from both rhesus and pigtailed macaques does not restrict HIV-1 infection and differ
107 from human CypA at only two amino acid positions [D66N and R69H], both of which are outside
108 the active site (Fig 1A) and differently affect binding to lentiviral capsids (34, 35). We first

109 generated cells expressing HA-tagged owl monkey TRIMCyp (omkTRIMCyp), or chimeric
110 proteins in which the CypA domain was replaced with human CypA (TRIM-huCypA) or human
111 CypA with D66N, R69H, or both D66N/R69H substitutions. We then challenged these cells with
112 HIV-1_{WT}, its derivatives encoding CA mutations with altered MX2-sensitivity, and other lentiviruses
113 (S1 Fig). Cells were also treated with the CypA inhibitor cyclosporine A (CsA) at the time of
114 infection to abolish CypA:CA interactions. As expected, HIV-1_{WT} infection was potently inhibited
115 (~200-fold) by TRIM-huCypA$_{D66N}$ and TRIM-huCypA$_{D66N/R69H}$ in a manner reversible by CsA
116 treatment, while TRIM-huCypA$_{R69H}$ was inactive against HIV-1_{WT}. With the exception of the
117 cyclophilin-binding loop mutant G89V, all HIV-1 CA mutants tested exhibited similar sensitivity to
118 the chimeric TRIM-huCypAs as the WT virus. HIV-2 on the other hand, was inhibited (~10-fold)
119 by TRIM-huCypA$_{D66N}$ and TRIM-huCypA$_{D66N/R69H}$, but not TRIM-huCypA$_{R69H}$, while SIVmac was
120 insensitive to all TRIMCyps since it does not bind cyclophilins (S1 Fig) (25, 36, 37).

121 To generate CypA mutant cell lines, we employed a CRISPR/Cas9-AAV-based gene
122 engineering approach to target the *PPIA* locus (S2A Fig). CypA knock-out cells were generated
123 by introduction of guide RNAs targeting intron 1 and exon 4, resulting in either a deletion of most
124 of the coding sequence or a frameshift mutation that abrogated expression (S2B Fig). To generate
125 point mutant cells, an AAV containing donor-DNA for homology-directed repair was introduced
126 with D66N and/or R69H mutations (S2A and S2C Fig). Single cell clones with the desired mutation
127 were confirmed by sequencing of both genomic DNA and mRNA. We then tested the ability of
128 CypA in control and point mutant clones to bind HIV-1 CA *in vitro* (S3 Fig), and found that both
129 CypA$_{WT}$ and CypA$_{R69H}$, but not CypA$_{D66N}$ or CypA$_{D66N/R69H}$ pelleted with WT or N57A mutant CA,
130 while CA(G89V) did not bind to CypA from any of the cell lines.

131 CypA mutant cell lines were then transduced with a lentiviral vector for doxycycline-
132 inducible expression of MX2 and infected with GFP-reporter viruses in the presence or absence
133 of CsA (Fig 1). CsA addition in HT1080 cells is known to reduce infection of HIV-1_{WT} and abolish
134 the antiviral activity of MX2 ((29) and Fig 1B). We observed similarly reduced levels of infectivity
135 and a lack of MX2 sensitivity in CypA$^{-/-}$, CypA$_{D66N}$, and CypA$_{D66N/R69H}$, but not CypA$_{R69H}$ cells.

136 Mutation or deletion of CypA had no effect on infection of the HIV-$1_{G89V\ CA}$, or on the slight
137 enhancement of infection by this mutant upon MX2 expression. We previously reported a dramatic
138 sensitivity of the cell-cycle-dependent and MX2-resistant HIV-$1_{N57S\ CA}$ to CsA addition that is
139 reversed by MX2 (29). Here we observed the same ~50-fold reduction in infectivity and rescue by
140 MX2 in CsA-treated and $CypA^{-/-}$, $CypA_{D66N}$, or $CypA_{D66N/R69H}$, but not $CypA_{R69H}$ cells (Fig 1B). Since
141 the N57A CA mutation was utilized for *in vitro* CA binding experiments, we also confirmed that
142 this mutant exhibited the same phenotype, as did the N57D mutation, although this mutant had
143 lower overall levels of infectivity which were slightly enhanced by MX2 even in the absence of
144 CsA treatment (S4 Fig). Infectivity and MX2 sensitivity of HIV-$1_{A92E\ CA}$, HIV-$1_{N74D\ CA}$, and HIV-1_{T210K}
145 $_{CA}$ in $CypA^{-/-}$, $CypA_{D66N}$, or $CypA_{D66N/R69H}$ cells also phenocopied CsA treatment in WT and
146 $CypA_{R69H}$ cells. Furthermore, no additional effects of CsA treatment on HIV-1_{WT} or CA mutant
147 infection were observed in CypA knock-out or mutant cell lines (Fig 1B and S4 Fig). Collectively,
148 these data demonstrate that the effect of CsA on HIV-1 infection and MX2 sensitivity are the direct
149 result of abrogating CA-CypA interactions and do not involve other cyclophilins, and further
150 suggests that they do not involve other cellular functions of CypA. However, since it is unknown
151 whether the conformational changes in CypA resulting from substitution at residue 66 affect
152 interactions between CypA and any of its cellular substrates, we cannot definitively exclude the
153 possibility that $CypA_{D66N}$ fails to isomerize a cellular substrate relevant for these interactions.
154 In contrast to HIV-1, HIV-2 sensitivity to MX2 is unaffected by CsA treatment ((29) and Fig
155 1B), although HIV-2 CA does interact with CypA with low affinity (34). The CypA D66N and R69H
156 mutations increase binding affinity, making HIV-2 sensitive to rhesus and pigtailed macaque
157 TRIMCyps ((34, 35, 37) and S1 Fig). On the other hand, huCypA interaction with SIVagmTAN do
158 not appear to involve CypA residues 66 or 69, as this virus was restricted by all TRIMCyp fusions
159 tested (although this virus is not restricted by owl monkey TRIMCyp with the NH mutation,
160 highlighting the complexity of lentiviral CA-CypA interactions (35)). However, both HIV-2 and
161 SIVagmTAN infection and MX2 sensitivity were unaffected in CypA-knockout and mutant cells,
162 similar to SIVmac, which does not bind cyclophilins, (Fig 1B and S4 Fig). These results indicate

163 that unlike restriction of HIV-1, inhibition of other primate lentiviruses by MX2 is independent of
164 CA-CypA interactions.
165
166 **Determinants for CA-specific effects of MX2 on lentivirus infection.** We next sought to
167 identify the determinants in MX2 that affect the CA- and CypA-specific sensitivity of lentiviruses
168 to MX2 activity. We expressed a panel of (C-terminally myc tagged) MX2 mutants that altered the
169 N-terminal CA-interacting domain, GTP binding and hydrolysis, or oligomerization (Fig 2) in HeLa
170 and HT1080 cells and first determined their effect on HIV-1_{WT} infection in the presence and
171 absence of CsA. Murine leukemia virus (MLV) was included as an MX2-insensitive negative
172 control. As expected (6, 7, 17, 21, 38), MX2 with a deletion of the N-terminal 25 amino acids
173 (ΔN25), mutation of the N-terminal triple-arginine motif ($RRR_{11-13}AAA$), or phosphomimetic
174 S14D/S17D/S18D ($SSS_{14,17,18}DDD$) did not inhibit HIV-1_{WT} infection, while chimeric MX1
175 expressing the N-terminal 91 amino acids of MX2 ($MX1_{MX2-NTD}$), and non-phosphorylatable
176 S14A/S17A/S18A ($SSS_{14,17,18}AAA$) had antiviral activity similar to WT MX2, that was abrogated in
177 the presence of CsA HT1080, but not HeLa cells (Fig 3 and S5 Fig). Both the monomeric M574D
178 and limited oligomer forming R455D mutants exhibited no anti-HIV-1 activity, while dimeric
179 $YRGK_{487-490}AAAA$ had extremely reduced antiviral activity in both HeLa and HT1080 cells. This is
180 in contrast with previous reports that have shown full antiviral activity of dimeric MX2 in U87-MG
181 and HOS cells (16, 18) and suggests that the requirements for MX2 oligomerization are cell-type
182 specific. The T151A mutant of MX2, which binds, but does not hydrolyze GTP (5), restricted HIV-
183 1 infection in both HeLa and HT1080 cells, confirming that GTPase activity is dispensable for anti-
184 HIV-1 activity (6, 7). The T151A mutant also restricted HIV-1_{WT} infection in the presence of CsA
185 in both cell lines. On the other hand, the GTP-binding mutant K131A, which retains anti-HIV-1
186 activity in K562, HOS, U87-MG (6, 7), and HeLa cells (S5 Fig), failed to inhibit infection in HT1080
187 cells, indicating that requirements for GTP binding are also cell-type specific. The requirement for
188 GTP binding is also virus-specific, since the K131A mutation abrogated antiviral activity against

189 HIV-2 and SIVmac, while all other MX2 mutants that inhibited HIV-1_{WT} infection also inhibited HIV-
190 2 and SIVmac infection.

191 In most cases, MX2 mutants that inhibited HIV-1_{WT} infection also enhanced HIV-$1_{G89V\ CA}$
192 infection in both HeLa and HT1080 cells, while those that did not inhibit the WT virus had no effect
193 on the G89V CA mutant virus (Fig 3 and S5 Fig). Similarly, only MX2 mutants that inhibited HIV-
194 1_{WT} infection ($MX1_{MX2\text{-}NTD}$ and $SSS_{14,17,18}AAA$) were able to reverse the reduction in HIV-$1_{N57S\ CA}$
195 infectivity in the presence of CsA in HT1080 cells. These data suggest that similar determinants
196 are involved in the antiviral activity of MX2, as well as the CA-specific, CypA-dependent pro-viral
197 effects of MX2. The $MX2_{T151A}$ mutant, however, was a notable exception to this trend in that it
198 failed to rescue HIV-$1_{N57S\ CA}$ infection in CsA-treated HT1080 cells, and inhibited HIV-$1_{G89V\ CA}$
199 infection in both HeLa and HT1080 cells. Thus, while CA-CypA interactions are required for the
200 full antiviral activity of WT MX2, MX2 which can bind but not hydrolyze GTP restricts HIV-1
201 infection even in the absence CypA.

202 We next tested the effects of GTPase-deficient MX2 on HIV infection in our CypA knock-
203 out and mutant cell lines. As expected, the $MX2_{T151A}$ mutant inhibited both HIV-1_{WT} and HIV-1_{G89V}
204 $_{CA}$ infection in the presence or absence of CsA in control, $CypA^{-/-}$, and all CypA mutant cell lines
205 (S6 Fig). Furthermore, $MX2_{T151A}$ failed to enhance HIV-$1_{N57S\ CA}$ infection in $CypA^{-/-}$, $huCypA_{D66N}$
206 and $CypA_{D66N/R69H}$ cells. Sensitivity of HIV-2 to both WT and T151A mutant MX2 was similar in all
207 cell lines, further demonstrating that CypA-interactions with HIV-2 CA do not affect MX2 sensitivity
208 (S6 Fig).

209 In 2022, Betancor, *et al.* (21) identified several serine and threonine residues of MX2 in
210 addition to positions 14, 17, and 18 whose phosphorylation state affects the antiviral activity and
211 substrate specificity of MX2. In particular, they found that MX2 T151 is phosphorylated, and
212 demonstrated that a phosphomimetic $MX2_{T151D}$ exhibited increased antiviral activity against HIV-
213 1_{WT} and conferred antiviral activity against the MX2-resistant HIV-$1_{N74D\ CA}$, HIV-$1_{P90A\ CA}$, and HIV-
214 $1_{T210K\ CA}$. To determine whether the ability of the $MX2_{T151A}$ mutant to restrict HIV-1 infection in the
215 absence of CypA-CA binding is due to the lack of a phosphate group at this residue or due to the

216 inability to hydrolyze GTP, we assessed the antiviral activity of the phosphomimetic T151D MX2
217 mutant in HT1080 and HeLa cells (Fig 4 and S7 Fig). $MX2_{T151D}$ exhibited increased antiviral
218 activity against HIV-1_{WT}, and to a smaller extent against HIV-2 and SIVmac in both cell types.
219 While the previous report indicated that MLV infection in U87-MG cells is sensitive to $MX2_{T151D}$,
220 we observed no restriction of MLV by this mutant. $MX2_{T151D}$ inhibited HIV-$1_{N57S\ CA}$ infection in both
221 HeLa and HT1080 cells, and only partially rescued infectivity of this mutant in CsA-treated
222 HT1080 cells (Fig 4 and S7 Fig). Finally, similar to $MX2_{T151A}$, $MX2_{T151D}$ inhibited HIV-1_{WT} infection
223 in the presence of CsA as well as infection of HIV-$1_{G89V\ CA}$, demonstrating that phosphorylation at
224 MX2 residue T151 does not determine CA-CypA-dependent antiviral activity of MX2. Collectively,
225 these results indicate that the inability to hydrolyze GTP abrogates the requirement for HIV-1 CA-
226 CypA interactions in the antiviral activity of MX2.
227
228 **Effect of GTPase domain-CA interactions on MX2 activity in the absence of CypA-CA**
229 **binding.** One possibility explaining the ability of T151A/D mutants of MX2 to inhibit HIV-1 infection
230 in the absence of CA-CypA interactions is that the lack of GTP hydrolysis facilitates interactions
231 between the viral CA and the CA-binding site of the GTPase domain (39). To address this
232 hypothesis, we constructed a number of MX2 mutants affecting GTPase activity (T151A), the N-
233 terminal triple arginine motif ($_{11}AAA_{13}$) and/or the CA-binding residues in the GTPase domain
234 [G184S, N260S, Q351E (SSE)] and assessed their antiviral activity (Fig 5 and S8 Fig). Mutation
235 of the triple arginine motif abrogated the antiviral activity of $MX2_{T151A}$ against HIV-1_{WT}, HIV-1_{G89V}
236 $_{CA}$, HIV-2, and SIVmac. On the other hand, mutation of the CA-binding residues of the GTPase
237 domain did not affect the antiviral activity of $MX2_{T151A}$ in the presence or absence of CsA against
238 these viruses; in fact, the SSE/T151A mutant appeared to have enhanced antiviral activity as
239 compared to WT or T151A MX2. Therefore, these CA-GTPase domain interactions do not
240 mediate the antiviral activity of GTPase-deficient MX2. Interestingly however, mutation of GTPase
241 domain-CA interacting residues did affect the enhancement of HIV-$1_{N57S\ CA}$ infection in CsA-
242 treated HT1080 cells, almost fully restoring the ability of $MX2_{T151A}$ to rescue HIV-$1_{N57S\ CA}$ infection,

243 suggesting that the lack of enhancement by $MX2_{T151A}$ under these conditions is at least partially
244 mediated by GTPase domain-CA interactions.

245 Next, we explored whether additional determinants affect the ability of the GTPase-
246 deficient MX2 to restrict infection of primate lentiviruses in the absence of CA-CypA binding. We
247 generated chimeric $MX1_{MX2\text{-}NTD}$ proteins with mutations corresponding to K131A (K83A) and
248 T151A/D (T103A/D), as well as mutations in MX1 alone as a control, expressed them in HT1080
249 and HeLa cells, and assessed their antiviral activity (Fig 6 and S9 Fig). Inhibition of HIV-2 and
250 SIVmac infection by chimeric $MX1_{MX2\text{-}NTD}$ was unaffected by all three mutations in both cell lines,
251 while GTP binding was required for restriction by MX2 (Fig 3 and S5 Fig). The effect of these
252 mutations on restriction of HIV-1_{WT} was cell-type specific, as $MX1_{MX2\text{-}NTD}$ chimeras restricted HIV-
253 1_{WT} infection in the presence or absence of CsA in HeLa cells but did not restrict HIV-1_{WT} in CsA-
254 treated HT1080 cells. The effects on HIV-$1_{G89V\ CA}$ infection were also cell-type specific, while
255 $MX1_{MX2\text{-}NTD}$ enhanced HIV-$1_{G89V\ CA}$ infection in both cell types, the K83A and T103A MX2 mutants
256 modestly restricted HIV-$1_{G89V\ CA}$ infection. Furthermore, the T103D MX2 mutant had no effect on
257 HIV-$1_{G89V\ CA}$ in HT1080 cells, while the opposite (no inhibition or enhancement by K83A and
258 T103A, restriction by T103D) was observed in HeLa cells. Finally, HIV-$1_{N57S\ CA}$ infection was not
259 inhibited by any $MX1_{MX2\text{-}NTD}$ chimeras in either cell type, and was rescued from the inhibitory effect
260 of CsA treatment in HT1080 cells by all three GTPase $MX1_{MX2\text{-}NTD}$ mutants. The effect of GTPase
261 mutations in $MX1_{MX2\text{-}NTD}$ chimeras on the HIV-$1_{N57S\ CA}$ mutant are in agreement with those shown
262 in Figure 5 regarding the role of CA-interacting residues in the GTPase domain. However, the
263 altered effects of GTP binding/hydrolysis mutant-$MX1_{MX2\text{-}NTD}$ chimeras on HIV-1_{WT}, HIV-$1_{G89V\ CA}$,
264 HIV-2, and SIVmac infection as compared to the K131A, T151A, and T151D mutants of MX2
265 demonstrate that additional unknown determinants in the GTPase, stalk, or L4 domain affect
266 interactions between MX2 and these viruses.

267

268 **Effects of Nup and NTR depletion on the antiviral activity of GTPase-deficient MX2.** Our
269 previous work demonstrated Nups mediate the antiviral activity of MX2 in a CA and CypA-

270 dependent manner (29). Since $MX2_{T151A}$ retains antiviral activity in the absence of CA-CypA
271 interactions, we next sought to determine whether this mutation also affected Nup/NTR
272 requirements for antiviral function. Using our previously validated siRNA library targeting Nups
273 and NTRs (Fig 7A and (29)), HT1080 cells were transfected with siRNA before being split into
274 replicated wells for $MX2_{WT}$ or $MX2_{T151A}$ induction (via doxycycline addition) followed by infection
275 with HIV-1_{WT} (S10 Fig). Knockdown of either RANBP2 or NUP153 abrogated the antiviral activity
276 of both $MX2_{WT}$ and $MX2_{T151A}$ against HIV-1_{WT} (Fig 7B-C). Furthermore, depletion of the Nup62
277 subcomplex, transmembrane, and nuclear basket Nups also had similar effects (eg. NUP62
278 depletion reduced $MX2_{WT}$ and $MX2_{T151A}$ activity, while NUP54, NUPL1, POM121, NDC1, NUP50,
279 and TPR depletion either increased antiviral activity or had no effect), indicating that the T151A
280 MX2 mutation does not completely alter MX2-Nup interactions. Moreover, the effects of NTR
281 depletion were similar, suggesting that abrogation of GTPase activity does not affect MX2-
282 transportin interactions. However, a number of differences were evident in the Nup requirements
283 for $MX2_{WT}$ and $MX2_{T151A}$ activity (eg. multiple components of the Nup107 and Nup93
284 subcomplexes reduced the antiviral activity of $MX2_{WT}$, but not $MX2_{T151A}$). Most notably, NUP88
285 and NUP214 depletion abolished the antiviral activity of $MX2_{WT}$, but not $MX2_{T151A}$.

286 We next investigated the effects of Nup depletion on the MX2 sensitivity of HIV-$1_{G89V\ CA}$.
287 As we previously reported (29), the increase in HIV-$1_{G89V\ CA}$ infectivity exerted by MX2 is amplified
288 by some Nup depletions (eg. NUP62, NUP88, NUP214, NUP153), and diminished by others (eg.
289 NUP155, NUP54, RANBP2) (Fig 7D). As expected, a number of Nup depletions also altered the
290 activity of $MX2_{T151A}$ against HIV-$1_{G89V\ CA}$ (Fig 7E). We observed no clear correlation between
291 whether a knockdown affected enhancement of HIV-$1_{G89V\ CA}$ infection by MX2 and whether it
292 caused loss of $MX2_{T151A}$ activity against HIV-$1_{G89V\ CA.}$ Depletion of transmembrane, cytoplasmic,
293 and nuclear basket Nups, as well as NTRs had similar effects on the antiviral activity of $MX2_{T151A}$
294 against both HIV-1_{WT} and HIV-$1_{G89V\ CA}$ (Fig 7C, E). Conversely, depletion of several Nups (SEC13,
295 NUP107, NUP133, NUP205, NUP155, NUP52, NUPL1) affected restriction of HIV-$1_{G89V\ CA}$ but not
296 HIV-1_{WT}, while only NUP98 knockdown reduced antiviral activity against HIV-1_{WT} but not HIV-1_{G89V}

297 $_{CA}$. Thus, these data indicate that the antiviral activity $MX2_{T151A}$ has distinct requirements for Nups
298 and NTRs, some of which are also affected by CA-CypA interactions.
299

300 **Discussion**

301 While the NTD of MX2 is of principal importance for viral substrate recognition and interaction
302 with cellular proteins (6, 9-13, 15, 17, 38), there is a growing appreciation for the importance of
303 the GTPase domain in MX2 function (21, 39, 40). Here, we demonstrate that the GTPase activity
304 of MX2 affects substrate specificity and nucleoporin requirements for anti-HIV-1 activity. While
305 WT MX2 does not restrict HIV-1 in the absence of CypA binding to CA, the T151A MX2 mutant,
306 which is able to bind, but not hydrolyze GTP (5), retains antiviral activity in the absence of CA-
307 CypA binding (Fig 3, S5 Fig, and S6 Fig). By generating cells containing endogenous mutations
308 in CypA that affect CA recognition, we demonstrate that the effects of CypA (and CsA treatment)
309 on HIV-1 and HIV-1 CA mutant infection and MX2 sensitivity are the direct result of interactions
310 with CA, and do not appear to involve interactions between CypA and other cellular proteins (Fig
311 1, S4 Fig, S6 Fig).

312 While the GTPase domain of MX2 has been found to directly bind the HIV-1 CA (39), we
313 found that these interactions were not involved in the CypA-independent activity of GTPase-
314 deficient MX2 (Fig 5 and S8 Fig). However, the antiviral activity of GTPase-deficient chimeric
315 $MX1_{MX2\text{-}NTD}$ fusions did not recapitulate the phenotype of the T151A mutant (Fig 6 and S9 Fig),
316 therefore there are additional determinants unique to MX2 that affect phosphorylation,
317 oligomerization/conformation, CA recognition, or interaction with other cellular proteins which alter
318 antiviral activity and substrate specificity. Importantly, we found that nucleoporin requirements of
319 the T151A MX2 mutant for antiviral activity were altered as compared to WT MX2 in both CypA-
320 dependent and -independent ways, suggesting that this mutation affects both antiviral substrate-
321 specificity, and interaction with nuclear pore complexes. Additionally, since MX2 also affects
322 nuclear import of some non-viral cargos, it will be of interest in future investigations to determine

323 whether the determinants identified here which affect viral specificity also alter inhibition of specific
324 nuclear import pathways.

325 Interestingly, restriction of HIV-2, SIVmac, and SIVagmTAN by MX2 does not involve CA-
326 CypA interactions ((29), Fig 1 and S4 Fig), and GTP hydrolysis is dispensable for inhibition of
327 HIV-2 and SIVmac by both MX2 and $MX1_{MX2\text{-}NTD}$ fusions (Fig 3 and 6, S5 Fig and S9 Fig).
328 Therefore, it is likely that recognition of HIV-1 and other primate lentiviruses by MX2 involve
329 distinct interactions with the capsid surface, consequently requiring distinct determinants. Indeed,
330 given the ability of MX2 to inhibit replication of highly divergent viruses, including herpesviruses
331 and flaviviruses (reviewed in (22)), it appears that we are just beginning to understand the
332 mechanisms regulating MX2 specify and activity.

333 We also identified here a number of MX2 determinants that are cell-type specific,
334 highlighting the importance of other cellular players in MX2 activity. While our previous
335 investigation found that the K131A mutant of MX2 which is unable to bind GTP (5), retains antiviral
336 activity (6, 7), here we found that this activity is cell-type dependent since this mutant is inactive
337 in HT1080 cells (Fig 3). We further find that the $YRGK_{487\text{-}490}AAAA$ mutant of MX2, has minimal
338 antiviral activity in either HT1080 or HeLa cells, demonstrating that the requirements for higher-
339 order oligomerization of MX2 are also cell-type dependent. While the MX2 stalk is the major driver
340 of oligomerization, the GTPase domain also exerts effects on MX2 conformation (40).
341 Biochemical studies have found that MX2 spontaneously forms helical assemblies that are
342 depolymerized into oligomers upon GTP binding; importantly, the T151A MX2 mutant also self-
343 assembles, however these assemblies are loosened, but not dissociated upon GTP binding (40).
344 Thus, conformational changes in MX2 may explain the expanded substrate-specificity of the
345 T151A mutant. Importantly, recent work has shown that the MX2 residue T151 is phosphorylated,
346 and that the phosphomimetic T151D mutant has increased antiviral activity (21). We recapitulated
347 this finding and additionally found that this mutant is also able to restrict HIV-1 infection in the
348 absence of CA-CypA interactions (Fig 4 and S7 Fig), indicating that the lack of phosphorylation
349 of the T151A mutant does not explain its expanded substrate specificity. While the T151D MX2

350 mutant is unlikely to bind GTP, as noted by Betancor, G. *et al*, the negative charge of the
351 phosphomimetic T151D mutant may resemble the GTP-bound T151A mutant, and both mutants
352 have distinct subcellular localization as compared to WT MX2 (21), they may both therefore exist
353 in a “loose helical assembly”. While high GTP concentrations within cells would suggest that MX2
354 exists in its GTP-bound non-assembled state (40), it is also possible that changes in the
355 phosphorylation state of T151 regulates MX2 conformation (and GTP binding), thereby affecting
356 interactions with both viral substrates and nuclear pore complexes.

357 In summary, this report highlights the importance of GTPase activity in modulation of the
358 substrate specificity of MX2 and further indicate that highly complex interactions between MX2
359 and its cellular environment determine antiviral activity. While we have focused specifically on
360 human MX2, the regulation of the antiviral activity of other MX proteins is similarly complex. Given
361 the importance of MX proteins in the innate immune responses of a highly divergent range of
362 vertebrate species (3), the evolution of *Mx* genes has likely been the result of complex selective
363 pressures balancing substrate breadth and specificity, as well as interaction with cellular partners.
364

365 **Materials and Methods**

366 **Plasmid construction**

367 **MX2**

368 MX1 and MX2 mutants with or without a C-terminal myc-tag were cloned into the doxycycline-
369 inducible vector pLKOΔ (13, 29) using *Sfi*I. MX2ΔN25, $MX2_{T151A}$, and $MX2_{K131A}$ were PCR
370 amplified from pCSIB expression vectors (6), $MX2_{G184S/N260S/Q351S}$ (SSE) and MX2-SSE_{T151A} were
371 synthesized as gBlock™ fragments [Integrated DNA Technologies (IDT)], other mutants were
372 generated via PCR mutagenesis using the oligos indicated in S1 Table.

373

374 **TRIM5-fusions**

375 An LHCX MLV vector (Clontech) was engineered to express the N-terminal domains (RIGN, B-
376 Box and coiled coil) from owl monkey (omk) TRIMCyp followed by an HA tag and cloning sites
377 (NotI/SalI) that allowed introduction of various proteins as described in (41, 42). The plasmids
378 generated expressed HA-TRIM5 N-terminus fused to the Cyclophilin A domain from owl monkey
379 TRIMCyp (omkTRIMCyp), the human Cyclophilin A protein (huCypA), or the human Cyclophilin
380 A protein with the D66N, R69H, or D66N/R69H (pigtail macaque TRIMCyp) mutations generated
381 by overlap PCR with the primers indicated in S1 Table.

382

383 **AAV donor**

384 To construct the pAAV-*PPIA* donor plasmids for the generation of CypA point mutant cell lines
385 (S2 Fig), a 1596bp region of the *PPIA* locus (bases 7161 to 8757 NCBI Reference Sequence:
386 NG_029697.1) was synthesized as a gBlock™ fragment (IDT) and inserted into the pAAV
387 packaging plasmid (Cell Bio Labs) using *Nhe*I and *Xho*I. The PAM site for crRNA 2 was mutated
388 from TGG to TGA and for crRNA 3 form CCA to CTA. A silent *Hpa*I site was introduced into intron
389 3 as shown in S2C Fig. The $CypA_{R69H}$ donor template was synthesized, then $CypA_{D66N}$ and
390 $CypA_{D66N/R69H}$ donors were generated via overlap PCR with the primers indicated in S1 Table.

391

392 **HIV-1 CA mutants**

393 HIV-1 GFP reporter viruses containing the N57A or N57D capsid mutation (HIV-1_{N57A} and HIV-
394 1_{N57D}) was generated by overlap PCR (primers listed in S1 Table) and insertion into pNHGCapNM
395 as described previously (31) using *Not*I and *Mlu*I sites.

396

397 **Cell lines**

398 HEK 293T, HeLa, and HT1080 cell lines were maintained in Dulbecco's Modified Eagles Medium
399 [(DMEM) Gibco] with 10% fetal calf serum (Gibco), gentamicin (Gibco), and Plasmocin®
400 prophlyactic (InvivoGen). Plasmocin® was not present in cultures during infection, transduction,
401 or transfection. Cells were purchased from ATCC and were assumed to be authenticated by their
402 supplier and were not further characterized. Cells were monitored quarterly for retroviral
403 contamination by SYBR-Green based PCR RT assay (43, 44) and tested for mycoplasma
404 contamination by MycoStrip® detection kit (InvivoGen). Derivatives of HeLa and HT1080 cells
405 containing doxycycline-inducible Mx2, or fusion proteins were generated by transduction with
406 LKO-derived lentiviral vectors (13) followed by selection in 1μg ml^{-1} puromycin (Sigma-Aldrich).
407 HeLa cells stably expressing TRIM fusions were generated by transduction with LHCX-derived
408 vectors followed by selection in 100μg ml^{-1} hygromycin B (Gibco). Vector stocks for transduction
409 were generated by co-transfection of 293T cells with a VSV-G expression plasmid, an HIV-1_{NL4-3}
410 Gag-Pol expression plasmid, and LKO-derived vector, or an MLV Gag-Pol expression plasmid
411 and an LHCX-derived vector using polyethyleneimine (PolySciences). Expression was induced in
412 pLKO transduced cell lines through an overnight treatment with 500ng/ml doxycycline hyclate
413 (Sigma-Aldrich) prior to challenge with retroviruses or retroviral vectors.

414

415 **Generation of CypA knock-out and mutant cell lines**

416 AAVs containing donor sequence for homology directed repair were generated by co-transfection
417 of 293T cells pAAV-*PPIA*, pAAV-RC (DJ), and pHelper (CellBio Labs) at a 1:1:1 ratio using
418 polyethyleneimine (PolySciences). Supernatant was collected 72hrs post-transfection. $1x10^5$

419 HT1080 cells in a 24-well plate were infected with 200µL of AAV-containing supernatant 4-6 hours
420 prior to reverse transfection with Cas9 ribonucleoprotein complexes (RNPs).
421
422 Custom Alt-R™ CRISPR Cas9 guide RNAs targeting the *PPIA* locus were designed using the IDT
423 website. RNPs containing crRNA 1, 2, or 3:tracerRNA duplexes were generated according to
424 manufacturer instructions: 1µL of 100 µM crRNA, 1µ of 100µM tracrRNA-ATTO™ 550 (IDT) in
425 98µL of Nuclease-Free Duplex Buffer (IDT) were heated at 98°C for 5min, then cooled to room
426 temperature. 15µL of annealed guide RNA oligos were mixed with 15µL of 1µM recombinant Cas9
427 (IDT) in 220µL of Opti-MEM media (Gibco) and incubated for 5min at room temperature,
428 complexes were used immediately or stored at -80°C. HT1080 cells were reverse transfected in
429 96-well plates with RNPs using RNAiMax (Thermo Fisher) according to manufacturer instructions,
430 transfection complexes containing 15µL of each RNP was mixed with 1.2µL of RNAiMax and
431 18.8µL of OptiMEM for 20mins at room temperature, followed by addition of $4x10^4$ cells/well. For
432 generation of point mutant cell lines, 1µM Alt-R™ HDR Enhancer V2 (IDT) was included. HT1080
433 cells were transfected with RNPs containing guides 1 and 3 to generate $CypA^{-/-}$ cells and guides
434 2 and 3 to generate CypA-mutant cells (S2 Fig). Control cells were transfected with RNPs
435 containing the IDT negative control crRNA. 16hours post-transfection, cells were transferred to a
436 24-well plate, and AAV infection/transduction was repeated after an additional 24-48hours.
437 Single-cell clones were then derived by limiting dilution.
438
439 $CypA^{-/-}$ clones were screened via western blotting, sequences of knock-out alleles were
440 determined following PCR amplification from genomic DNA using (In1 F2 and In4 R primers),
441 followed by cloning into pCR-Blunt II TOPO [Zero Blunt™ TOPO™ kit (Thermo Fisher)], and
442 sequencing ≥3 clones from each cell line. CypA point mutant clones were screened via PCR
443 amplification from genomic DNA using (In1 F and In4 R2 primers) followed by *Hpa*I digestion.
444 Candidates were confirmed by PCR and sequencing from both genomic DNA and cDNA [using

445 SuperScript^{TM} III Reverse Transcriptase (Thermo Fisher)]. Genomic DNA and mRNA were
446 extracted using NucleoSpin Tissue and NucleoSpin RNA kits (Macherey-Nagel), respectively.
447
448 **Viruses**
449 All viruses were generated by transfection of 293T cells using polyethyleneimine (PolySciences).
450 GFP reporter proviral plasmids HIV-1_{NL4-3}ΔEnv-GFP (HIV-1, HIV-1_{G89V}, HIV-1_{A92E}, and G94D CA
451 mutants (45)), NHGCapNM (wild-type, HIV-1_{N57S}, HIV-1_{N57A}, HIV-1_{N57D}, HIV-1_{N74D}, G208R, and
452 HIV-1_{T210K} CA mutants (this investigation and (29, 31)), HIV-2_{ROD}ΔEnv-GFP, SIV_{MAC}ΔEnv-GFP,
453 SIV_{AGM}TANΔEnv-GFP (46) 10µg of proviral plasmid was co-transfected with 1µg of VSV-G
454 expression plasmid. For MLV, EIAV, and FIV, three plasmid vector systems (47-50) were also
455 used to generate GFP reporter viruses, whereby 5µg of Gag-Pol, 5µg of packeagable genome,
456 and 1µg of VSV-G expression plasmids were co-transfected. Levels of reverse transcriptase in
457 viral stocks were quantified using a one-step SYBR-Green based PCR RT assay as previously
458 described (43, 44).
459
460 **Infection assays**
461 Infectivity was measured in HeLa or HT1080 cells seeded in 96-well plates at 5 x 10^3 cells per
462 well and inoculated with serial-dilutions of VSV-G pseudotyped GFP reporter viruses in the
463 presence of 4µg ml^{-1} polybrene (Sigma-Aldrich). Where indicated, cyclosporine A (Sigma-Aldrich)
464 was added to the cultures at the time of infection at 5µM. Infected cells (%GFP positive of viable
465 cells) were enumerated by FACS analysis using an Attune NxT coupled to an Autosampler
466 (Invitrogen).
467
468 **CA-binding assay with HIV-1 CA tubes**
469 CA(WT), CA(G89V), and CA(N57A) were expressed from pET3a in BL21-DE3 cells and purified
470 as previously described (51-53). CA nanotubes were assembled in a high-ionic strength buffer
471 (15 mM Tris-HCl, pH 8.0; 2 M NaCl) as described (54, 55). Binding assays with HIV-1 CA

472 nanotubes were performed as described (29). In brief, control and CypA mutant HT1080 cells
473 were lysed by adding a passive lysis buffer (Promega) supplemented with protease inhibitor
474 cocktail (Roche). NaCl concentration in lysates was adjusted to 2 M and lysates were centrifuged
475 at 13,000 x g for 2 min at 4 ℃. Then the supernatant of the cell lysates was added to the preformed
476 CA nanotubes and incubated at room temperature for 30 min. Following centrifugation at 13,000
477 x g for 2 min at 4 ℃, the supernatant was saved, and the pellet was washed three times with the
478 high-ionic strength buffer. LDS Reducing Sample buffer (Thermo Scientific Chemicals) was added
479 to both pulled-down and unbound fractions, and they were subjected to SDS-PAGE. The proteins
480 of interest were detected by immunoblotting using respective antibodies.
481

482 **RNA interference**

483 RNA interference using a custom siRNA library (Table 1) targeting Nups and NTRs was performed
484 as previously described (29). HT1080 cells stably transduced with doxycycline-inducible MX2 or
485 $MX2_{T151A}$ were reverse transfected with 25pmol of siRNA (Table 2; SMARTpool, Dharmacon)
486 using Lipofectamine RNAiMax (Invitrogen) at a concentration of 5 x 10^4 cells/ml in 12-well plates.
487 Non-transfected cells, transfection reagent alone, and non-targeting siRNA were used as controls,
488 no significant difference in viral infectivity or Mx2-restriction were observed for each of these
489 controls, as such, for each experiment, only the non-targeting siRNA control is shown. 24 hours
490 after transfection, cells were trypsinized, diluted 1:2.5 and re-plated in 96-well plates and treated
491 with doxycycline, followed by infection with GFP reporter viruses 36-48h later (See Figure S10B).

Table 1. ON-TARGET SMARTpool siRNA utilized in this investigation

Gene Symbol	Gene ID
AAAS	8086
AHCTF1	25909
CPSF6	11052
GLE1	2733
IPO11	51194
IPO13	9670
IPO4	79711
IPO5	3843
IPO7	10527
IPO8	10526
IPO9	55705
KPNA1	3836
KPNA2	3838

KPNA3	3839
KPNA4	3840
KPNA5	3841
KPNA6	23633
KPNB1	3837
NDC1	55706
NUP107	57122
NUP133	55746
NUP153	9972
NUP155	9631
NUP160	23279
NUP188	23511
NUP205	23165
NUP210	23225
NUP214	8021
NUP35	129401
NUP37	79023
NUP43	348995
NUP50	10762
NUP54	53371
NUP62	23636
NUP85	79902
NUP88	4927
NUP93	9688
NUP98	4928
NUPL1	9818
POM121	9883
PPIA	5478
RAE1	8480
RANBP2	5903
SEC13	6396
SEH1L	81929
TNPO1	3842
TNPO2	30000
TNPO3	23534
TPR	7175

492

493 **Western blotting**

494 Cell suspensions were lysed in NuPage LDS (Invitrogen) or SDS sample buffer, followed by
495 sonication, and separated by electrophoresis on NuPage 4-12% Bis-Tris gels (Invitrogen) and
496 blotted onto polyvinylidene fluoride (PDVF, BioRad Laboratories). Membranes were incubated
497 with the antibodies listed in Table 2, followed by incubation with goat anti-rabbit-HRP or goat anti-
498 mouse-HRP secondary antibodies (Jackson ImmunoResearch). SeeBlue Plus2 and MagicMark
499 XP Pre-stained Protein Standards (Thermo Fisher) were used. Blots were developed with
500 SuperSignal West Femto Maximum Sensitivity Substrate (Thermo Fisher) and imaged on a C-
501 Digit scanner (LI-COR Biosciences).

Table 2. Antibodies utilized in this investigation

Reactivity	Species	Company	Catalog Number
GAPDH	mouse	Santa Cruz	sc-47724
HIV-1 p55+p24+p17	rabbit	Abcam	ab63917
MX2	rabbit	Novus Biologicals	NBP1-8108
Myc tag	mouse	Millipore	05-724

CypA	rabbit	Proteintech	10720-1-AP
HA tag	Mouse	BioLegend	901514
Tubulin	mouse	Sigma-Aldrich	T6074

502

503 **Statistical analyses**

504 Statistical significance was determined using GraphPad software (two-way ANOVA). Statistical
505 analyses for all figures are included in S1 File.

506

507 **Acknowledgements**

508 We thank Dr. Kevin McCarthy for support, consultation, and assistance in generation of PyMOL
509 images; Mariah Cashbaugh and Ananya Venbakkam for technical support. Color-blind safe
510 "muted" qualitative color schemes from Paul Tol were used for figures (56). This work was
511 supported by grants from the NIH: R01AI1621172 (to M.Kane), R01 AI162665 (to M.K.), and the
512 Gilead Sciences Research Scholars Award (to M.Kane). The content is solely the responsibility
513 of the authors and does not necessarily represent the official views of the National Institutes of
514 Health or of Gilead Sciences.

515

516 **Author contributions**

517 Conceptualization: M.Kane.; Investigation: B.L., R.G., H.F., S.H., R.Z.Z., and M.Kane; Formal
518 Analysis and Visualization: M.Kane; Methodology: S.H., M.K., M.Kane; Funding Acquisition:
519 M.Kane; Writing – Original Draft Preparation: M.Kane.; Writing – Review and Editing: R.Z., M.K.,
520 and M.Kane.

521

522 **Declaration of interests**

523 The authors declare no competing interests.

524

525 1. Schoggins JW, Wilson SJ, Panis M, Murphy MY, Jones CT, Bieniasz P, et al. A diverse
526 range of gene products are effectors of the type I interferon antiviral response. Nature.
527 2011;472(7344):481-5.
528 2. Stetson DB, Medzhitov R. Type I interferons in host defense. Immunity. 2006;25(3):373-
529 81.
530 3. Haller O, Staeheli P, Schwemmle M, Kochs G. Mx GTPases: dynamin-like antiviral
531 machines of innate immunity. Trends in microbiology. 2015;23(3):154-63.
532 4. Melen K, Keskinen P, Ronni T, Sareneva T, Lounatmaa K, Julkunen I. Human MxB
533 protein, an interferon-alpha-inducible GTPase, contains a nuclear targeting signal and is localized
534 in the heterochromatin region beneath the nuclear envelope. The Journal of biological chemistry.
535 1996;271(38):23478-86.
536 5. King MC, Raposo G, Lemmon MA. Inhibition of nuclear import and cell-cycle progression
537 by mutated forms of the dynamin-like GTPase MxB. Proceedings of the National Academy of
538 Sciences of the United States of America. 2004;101(24):8957-62.
539 6. Kane M, Yadav SS, Bitzegeio J, Kutluay SB, Zang T, Wilson SJ, et al. MX2 is an interferon-
540 induced inhibitor of HIV-1 infection. Nature. 2013;502(7472):563-6.
541 7. Goujon C, Moncorge O, Bauby H, Doyle T, Ward CC, Schaller T, et al. Human MX2 is an
542 interferon-induced post-entry inhibitor of HIV-1 infection. Nature. 2013;502(7472):559-62.
543 8. Liu Z, Pan Q, Ding S, Qian J, Xu F, Zhou J, et al. The interferon-inducible MxB protein
544 inhibits HIV-1 infection. Cell host & microbe. 2013;14(4):398-410.
545 9. Crameri M, Bauer M, Caduff N, Walker R, Steiner F, Franzoso FD, et al. MxB is an
546 interferon-induced restriction factor of human herpesviruses. Nat Commun. 2018;9(1):1980.
547 10. Schilling M, Bulli L, Weigang S, Graf L, Naumann S, Patzina C, et al. Human MxB Protein
548 Is a Pan-herpesvirus Restriction Factor. Journal of virology. 2018;92(17).
549 11. Yi DR, An N, Liu ZL, Xu FW, Raniga K, Li QJ, et al. Human MxB Inhibits the Replication
550 of Hepatitis C Virus. Journal of virology. 2019;93(1).
551 12. Matreyek KA, Wang W, Serrao E, Singh PK, Levin HL, Engelman A. Host and viral
552 determinants for MxB restriction of HIV-1 infection. Retrovirology. 2014;11:90.
553 13. Busnadiego I, Kane M, Rihn SJ, Preugschas HF, Hughes J, Blanco-Melo D, et al. Host
554 and viral determinants of Mx2 antiretroviral activity. Journal of virology. 2014;88(14):7738-52.
555 14. Liu Z, Pan Q, Liang Z, Qiao W, Cen S, Liang C. The highly polymorphic cyclophilin A-
556 binding loop in HIV-1 capsid modulates viral resistance to MxB. Retrovirology. 2015;12:1.
557 15. Fricke T, White TE, Schulte B, de Souza Aranha Vieira DA, Dharan A, Campbell EM, et
558 al. MxB binds to the HIV-1 core and prevents the uncoating process of HIV-1. Retrovirology.
559 2014;11:68.
560 16. Fribourgh JL, Nguyen HC, Matreyek KA, Alvarez FJ, Summers BJ, Dewdney TG, et al.
561 Structural insight into HIV-1 restriction by MxB. Cell host & microbe. 2014;16(5):627-38.
562 17. Goujon C, Moncorge O, Bauby H, Doyle T, Barclay WS, Malim MH. Transfer of the amino-
563 terminal nuclear envelope targeting domain of human MX2 converts MX1 into an HIV-1 resistance
564 factor. Journal of virology. 2014;88(16):9017-26.
565 18. Dicks MD, Goujon C, Pollpeter D, Betancor G, Apolonia L, Bergeron JR, et al.
566 Oligomerization Requirements for MX2-Mediated Suppression of HIV-1 Infection. Journal of
567 virology. 2016;90(1):22-32.
568 19. Mitchell PS, Patzina C, Emerman M, Haller O, Malik HS, Kochs G. Evolution-guided
569 identification of antiviral specificity determinants in the broadly acting interferon-induced innate
570 immunity factor MxA. Cell host & microbe. 2012;12(4):598-604.
571 20. Betancor G, Jimenez-Guardeno JM, Lynham S, Antrobus R, Khan H, Sobala A, et al.
572 MX2-mediated innate immunity against HIV-1 is regulated by serine phosphorylation. Nat
573 Microbiol. 2021;6(8):1031-42.
574 21. Betancor G, Bangham M, Jeon JK, Shah K, Lynham S, Jimenez-Guardeno JM, et al. MX2
575 Viral Substrate Breadth and Inhibitory Activity Are Regulated by Protein Phosphorylation. mBio.
576 2022;13(4):e0171422.
577 22. Betancor G. You Shall Not Pass: MX2 Proteins Are Versatile Viral Inhibitors. Vaccines
578 (Basel). 2023;11(5).

579 23. Campbell EM, Hope TJ. HIV-1 capsid: the multifaceted key player in HIV-1 infection.
580 Nature reviews Microbiology. 2015;13(8):471-83.
581 24. De Iaco A, Luban J. Cyclophilin A promotes HIV-1 reverse transcription but its effect on
582 transduction correlates best with its effect on nuclear entry of viral cDNA. Retrovirology.
583 2014;11:11.
584 25. Schaller T, Ocwieja KE, Rasaiyaah J, Price AJ, Brady TL, Roth SL, et al. HIV-1 capsid-
585 cyclophilin interactions determine nuclear import pathway, integration targeting and replication
586 efficiency. PLoS pathogens. 2011;7(12):e1002439.
587 26. Kim K, Dauphin A, Komurlu S, McCauley SM, Yurkovetskiy L, Carbone C, et al. Cyclophilin
588 A protects HIV-1 from restriction by human TRIM5alpha. Nat Microbiol. 2019;4(12):2044-51.
589 27. Selyutina A, Persaud M, Simons LM, Bulnes-Ramos A, Buffone C, Martinez-Lopez A, et
590 al. Cyclophilin A Prevents HIV-1 Restriction in Lymphocytes by Blocking Human TRIM5alpha
591 Binding to the Viral Core. Cell Rep. 2020;30(11):3766-77 e6.
592 28. Yamashita M, Engelman AN. Capsid-Dependent Host Factors in HIV-1 Infection. Trends
593 in microbiology. 2017;25(9):741-55.
594 29. Kane M, Rebensburg SV, Takata MA, Zang TM, Yamashita M, Kvaratskhelia M, et al.
595 Nuclear pore heterogeneity influences HIV-1 infection and the antiviral activity of MX2. Elife.
596 2018;7.
597 30. Miles RJ, Kerridge C, Hilditch L, Monit C, Jacques DA, Towers GJ. MxB sensitivity of HIV-
598 1 is determined by a highly variable and dynamic capsid surface. Elife. 2020;9.
599 31. Rihn SJ, Wilson SJ, Loman NJ, Alim M, Bakker SE, Bhella D, et al. Extreme genetic
600 fragility of the HIV-1 capsid. PLoS pathogens. 2013;9(6):e1003461.
601 32. Flaherty P, Jain P. Peptidyl Prolyl Isomerase Inhibitors. In: Macor JE, editor. Annual
602 Reports in Medicinal Chemistry. 46: Elsevier Inc.; 2011. p. 337-49.
603 33. Wang P, Heitman J. The cyclophilins. Genome Biol. 2005;6(7):226.
604 34. Price AJ, Marzetta F, Lammers M, Ylinen LM, Schaller T, Wilson SJ, et al. Active site
605 remodeling switches HIV specificity of antiretroviral TRIMCyp. Nat Struct Mol Biol.
606 2009;16(10):1036-42.
607 35. Virgen CA, Kratovac Z, Bieniasz PD, Hatziioannou T. Independent genesis of chimeric
608 TRIM5-cyclophilin proteins in two primate species. Proceedings of the National Academy of
609 Sciences of the United States of America. 2008;105(9):3563-8.
610 36. Sayah DM, Sokolskaja E, Berthoux L, Luban J. Cyclophilin A retrotransposition into TRIM5
611 explains owl monkey resistance to HIV-1. Nature. 2004;430(6999):569-73.
612 37. Wilson SJ, Webb BL, Ylinen LM, Verschoor E, Heeney JL, Towers GJ. Independent
613 evolution of an antiviral TRIMCyp in rhesus macaques. Proceedings of the National Academy of
614 Sciences of the United States of America. 2008;105(9):3557-62.
615 38. Goujon C, Greenbury RA, Papaioannou S, Doyle T, Malim MH. A triple-arginine motif in
616 the amino-terminal domain and oligomerization are required for HIV-1 inhibition by human MX2.
617 Journal of virology. 2015;89(8):4676-80.
618 39. Betancor G, Dicks MDJ, Jimenez-Guardeno JM, Ali NH, Apolonia L, Malim MH. The
619 GTPase Domain of MX2 Interacts with the HIV-1 Capsid, Enabling Its Short Isoform to Moderate
620 Antiviral Restriction. Cell Rep. 2019;29(7):1923-33 e3.
621 40. Alvarez FJD, He S, Perilla JR, Jang S, Schulten K, Engelman AN, et al. CryoEM structure
622 of MxB reveals a novel oligomerization interface critical for HIV restriction. Sci Adv.
623 2017;3(9):e1701264.
624 41. Matreyek KA, Yucel SS, Li X, Engelman A. Nucleoporin NUP153 phenylalanine-glycine
625 motifs engage a common binding pocket within the HIV-1 capsid protein to mediate lentiviral
626 infectivity. PLoS pathogens. 2013;9(10):e1003693.
627 42. Schmidt F, Keele BF, Del Prete GQ, Voronin D, Fennessey CM, Soll S, et al. Derivation
628 of simian tropic HIV-1 infectious clone reveals virus adaptation to a new host. Proceedings of the
629 National Academy of Sciences of the United States of America. 2019;116(21):10504-9.
630 43. Del Prete GQ, Keele BF, Fode J, Thummar K, Swanstrom AE, Rodriguez A, et al. A single
631 gp120 residue can affect HIV-1 tropism in macaques. PLoS pathogens. 2017;13(9):e1006572.

632 44. Pizzato M, Erlwein O, Bonsall D, Kaye S, Muir D, McClure MO. A one-step SYBR Green
633 I-based product-enhanced reverse transcriptase assay for the quantitation of retroviruses in cell
634 culture supernatants. J Virol Methods. 2009;156(1-2):1-7.
635 45. Hatziioannou T, Cowan S, Von Schwedler UK, Sundquist WI, Bieniasz PD. Species-
636 specific tropism determinants in the human immunodeficiency virus type 1 capsid. Journal of
637 virology. 2004;78(11):6005-12.
638 46. Hatziioannou T, Cowan S, Goff SP, Bieniasz PD, Towers GJ. Restriction of multiple
639 divergent retroviruses by Lv1 and Ref1. The EMBO journal. 2003;22(3):385-94.
640 47. Kemler I, Barraza R, Poeschla EM. Mapping the encapsidation determinants of feline
641 immunodeficiency virus. Journal of virology. 2002;76(23):11889-903.
642 48. Mitrophanous K, Yoon S, Rohll J, Patil D, Wilkes F, Kim V, et al. Stable gene transfer to
643 the nervous system using a non-primate lentiviral vector. Gene therapy. 1999;6(11):1808-18.
644 49. Soneoka Y, Cannon PM, Ramsdale EE, Griffiths JC, Romano G, Kingsman SM, et al. A
645 transient three-plasmid expression system for the production of high titer retroviral vectors.
646 Nucleic acids research. 1995;23(4):628-33.
647 50. Neil S, Martin F, Ikeda Y, Collins M. Postentry restriction to human immunodeficiency
648 virus-based vector transduction in human monocytes. Journal of virology. 2001;75(12):5448-56.
649 51. Hung M, Niedziela-Majka A, Jin D, Wong M, Leavitt S, Brendza KM, et al. Large-scale
650 functional purification of recombinant HIV-1 capsid. PLoS One. 2013;8(3):e58035.
651 52. Pornillos O, Ganser-Pornillos BK, Banumathi S, Hua Y, Yeager M. Disulfide bond
652 stabilization of the hexameric capsomer of human immunodeficiency virus. J Mol Biol.
653 2010;401(5):985-95.
654 53. Pornillos O, Ganser-Pornillos BK, Kelly BN, Hua Y, Whitby FG, Stout CD, et al. X-ray
655 structures of the hexameric building block of the HIV capsid. Cell. 2009;137(7):1282-92.
656 54. Cortines JR, Monroe EB, Kang S, Prevelige PE, Jr. A retroviral chimeric capsid protein
657 reveals the role of the N-terminal beta-hairpin in mature core assembly. J Mol Biol.
658 2011;410(4):641-52.
659 55. Larue R, Gupta K, Wuensch C, Shkriabai N, Kessl JJ, Danhart E, et al. Interaction of the
660 HIV-1 intasome with transportin 3 protein (TNPO3 or TRN-SR2). The Journal of biological
661 chemistry. 2012;287(41):34044-58.
662 56. Tol P. Colour Schemes. 2021.
663 57. Fontoura BM, Blobel G, Matunis MJ. A conserved biogenesis pathway for nucleoporins:
664 proteolytic processing of a 186-kilodalton precursor generates Nup98 and the novel nucleoporin,
665 Nup96. J Cell Biol. 1999;144(6):1097-112.
666 58. Rosenblum JS, Blobel G. Autoproteolysis in nucleoporin biogenesis. Proc Natl Acad Sci
667 U S A. 1999;96(20):11370-5.
668 59. Pitossi F, Blank A, Schroder A, Schwarz A, Hussi P, Schwemmle M, et al. A functional
669 GTP-binding motif is necessary for antiviral activity of Mx proteins. Journal of virology.
670 1993;67(11):6726-32.
671 60. Ponten A, Sick C, Weeber M, Haller O, Kochs G. Dominant-negative mutants of human
672 MxA protein: domains in the carboxy-terminal moiety are important for oligomerization and
673 antiviral activity. Journal of virology. 1997;71(4):2591-9.
674

675

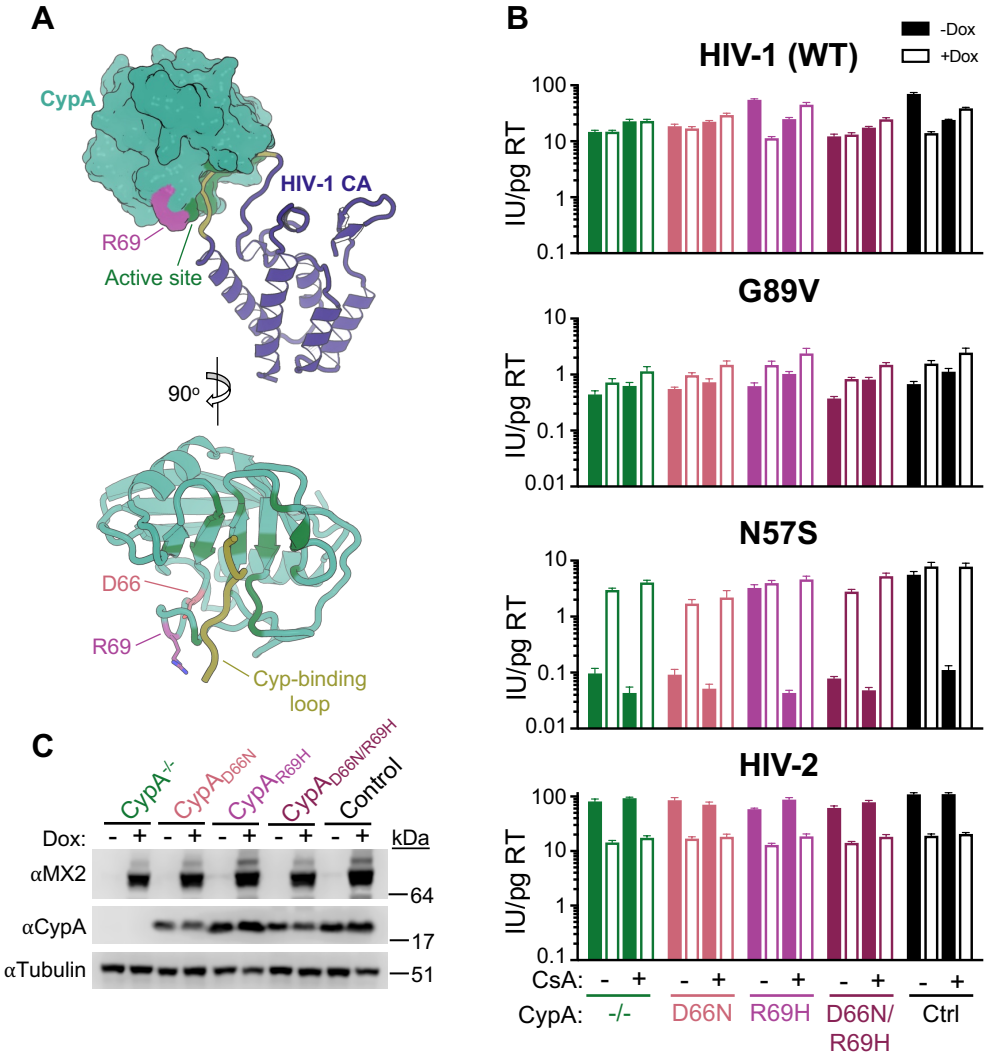

Figure 1. The effects of CsA on HIV-1 sensitivity to MX2 are the direct result of blocking CA-CypA interactions.

A) Structure of an HIV-1 capsid monomer in complex with CypA (PDB 1AK4). Critical active -site residues that interact with CA are indicated in dark green, amino acids outside the active site that affect capsid recognition highlighted in pink/magenta. The cyclophilin-binding loop of HIV-1 CA indicated in yellow.

B) Infection of control or CypA-mutant HT1080 cells expressing doxycycline-inducible MX2 in the presence (open bars) or absence (filled bars) of doxycycline (Dox) and present or absence of CsA with the indicated GFP reporter viruses. Titers are represented as mean + sem of infectious units (IU) per pg of reverse transcriptase (RT), n≥6 technical replicates combined from two-three independent experiments. Statistical analysis in S1 File.

C) Western blot analysis of doxycycline-inducible MX2, CypA, and tubulin loading control.

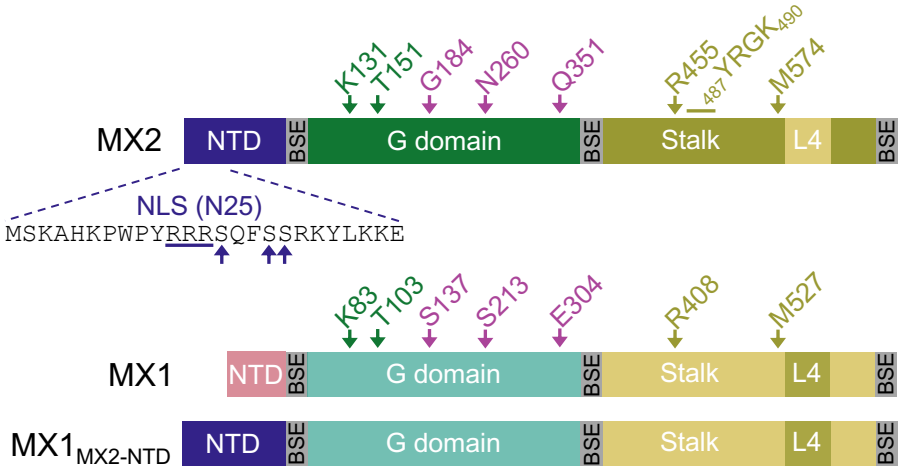

C

Residues/mutation	Function/effect of mutation	References
N91	N-terminal domain Can confer antiviral activity to heterologous proteins	(13, 17, 29)
N25	NPC targeting CA binding	(5-7, 15, 16)
$RRR_{11\text{-}13}$	Interaction with MLCP CA recognition	(15, 20, 38, 39)
$SSS_{14,17,18}$	Phosphorylation suppresses function and reduces NPC localization $AAA_{14,17,18}$ - Non-phosphorylatable $DDD_{14,17,18}$ - Phosphomimetic	(20)
T151	GTPase activity Phosphorylation affects antiviral activity and specificity T151A – No GTP hydrolysis, non-phosphorylatable T151D – Predicted to not bind GTP, phosphomimetic Corresponds to MX1 T103	(5, 21, 59, 60)
K131A	No GTP Binding Corresponds to MX1 K83	(5)
M574D	Monomeric Corresponds to MX1 M527	(18)
R455D	Limited oligomerization Corresponds to MX1 R408	(18)
$YRGK_{487\text{-}490}$-AAAA	Dimeric	(16, 18)
G184/N260/Q351	CA binding Correspond to MX1 S137/S213/E304	(38)

Figure 2. Summary of MX1 and MX2 mutants used in this study.

A) Diagram representing the various domains of MX2, with the N-terminal 25 amino acids shown in detail. BSE: bundle-signaling element. Residues of particular interest are indicated.

B) Diagram representing the domains of MX1 (top), with residues corresponding to those highlighted in MX2 indicated, and diagram of chimeric fusion of MX1 containing the N-terminal 91 amino acids of MX2 (bottom).

C) Overview of mutations in MX2 known to affect CA-binding, phosphorylation, GTPase activity, and oligomerization. Known consequences of mutations/functions of specific residues and relevant citations are shown.

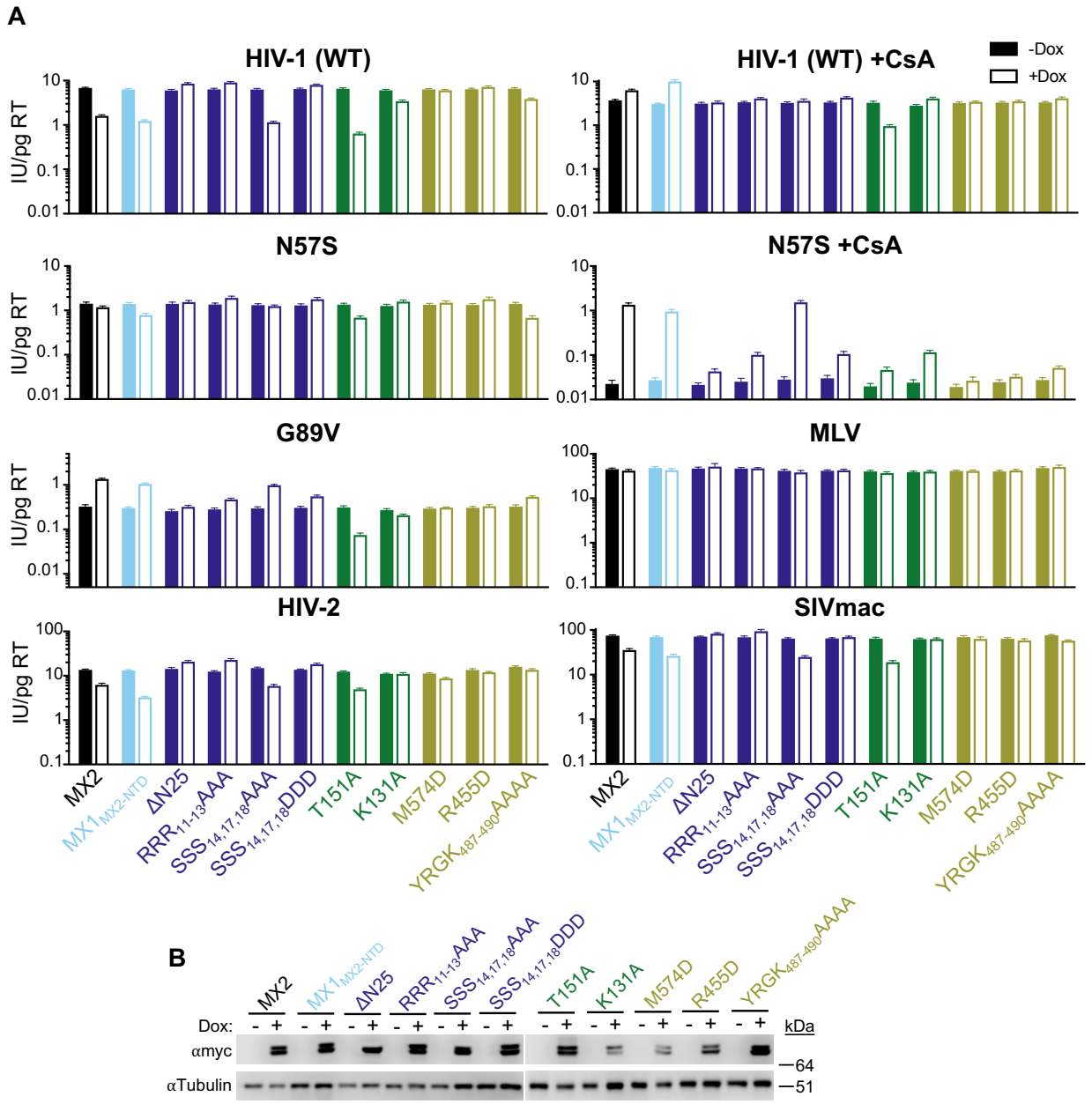

Figure 3. Determinants for MX2 activity in the absence of CA-CypA interactions.

A) Infectivity of GFP reporter viruses in HT1080 cells expressing doxycycline-inducible C-terminally myc-tagged MX2, MX2 mutants, or $MX1_{MX2\text{-}NTD}$ in the presence (open bars) and absence (filled bars) of doxycycline (Dox). Cells were infected in the presence of CsA where indicated. Titers are represented as mean + sem of infectious units (IU) per pg of reverse transcriptase (RT), n≥8 technical replicates combined from two-six independent experiments. Statistical analysis in S1 File.

B) Western blot analysis of doxycycline-inducible MX2-myc and tubulin loading control.

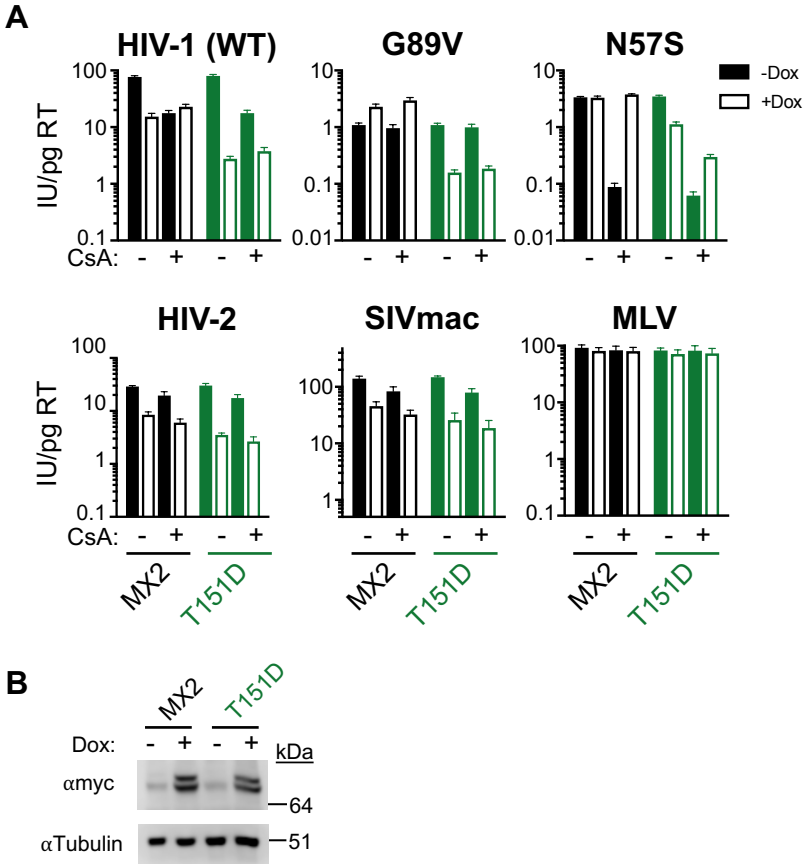

Figure 4. Phosphorylation at residue T151 does not determine CypA-independent MX2 activity.

A) Infection HT1080 cells stably transduced with doxycycline-inducible myc-tagged MX2 or $MX2_{T151D}$ in the presence (open bars) or absence (filled bars) of doxycycline and presence or absence of CsA with the indicated GFP reporter viruses. Titers are represented as mean + sem of infectious units (IU) per pg of reverse transcriptase (RT), n≥9 technical replicates combined from three-five independent experiments. Statistical analysis in S1 File.

B) Western blot analysis of doxycycline-inducible MX2-myc and tubulin loading control.

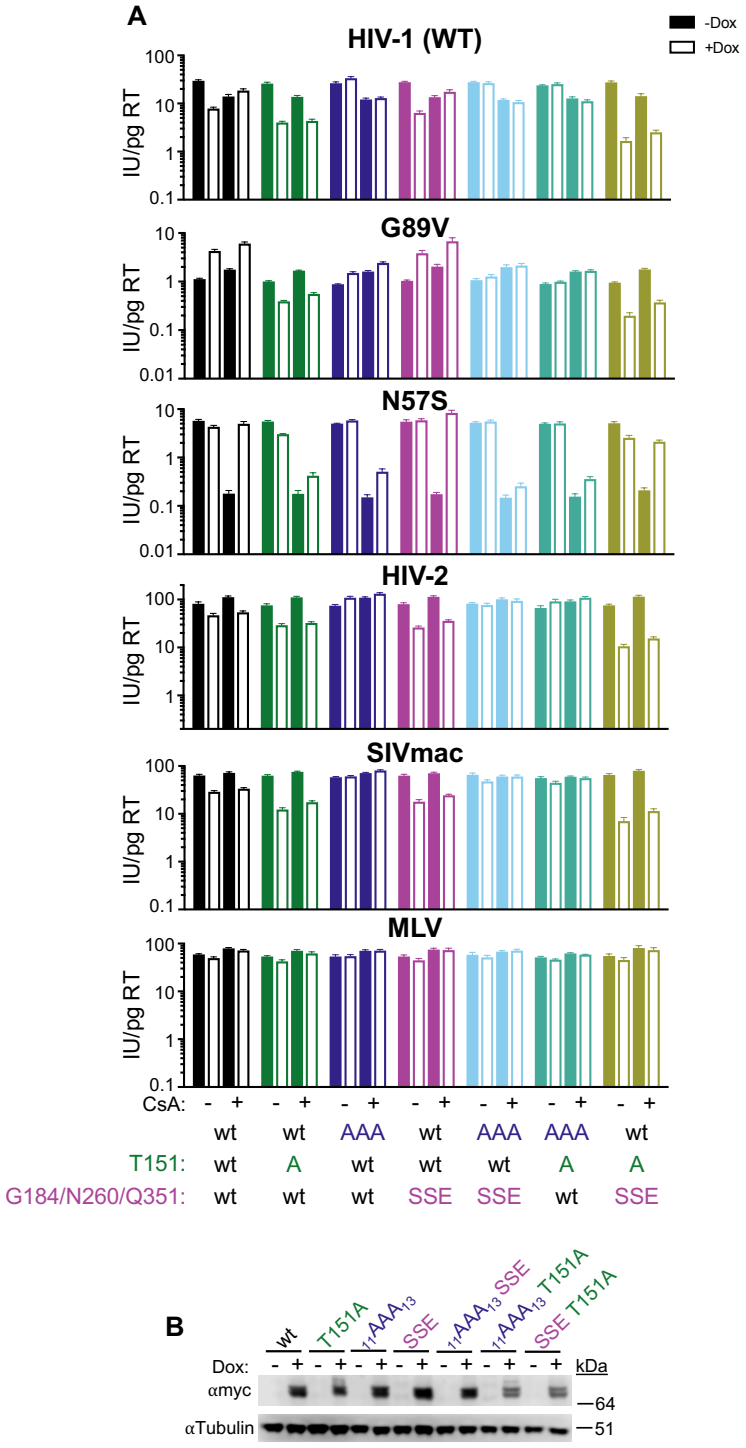

Figure 5. Restriction by GTPase-deficient MX2 in the absence of CA-CypA binding is not mediated by known CA-GTPase domain interactions.

A) Infection of HT1080 cells stably transduced with doxycycline-inducible myc-tagged MX2 with or without mutations in the N-terminal triple-arginine motif ($_{11}AAA_{13}$), T151A, or CA-binding residues in the GTPase domain (SSE) in the presence (open bars) or absence (filled bars) of doxycycline and presence or absence of CsA with the indicated GFP reporter viruses. Titers are represented as mean + sem of infectious units (IU) per pg of reverse transcriptase (RT), n≥9 technical replicates combined from three-five independent experiments. Statistical analysis in S1 File.

B) Western blot analysis of doxycycline-inducible MX2-myc and tubulin loading control.

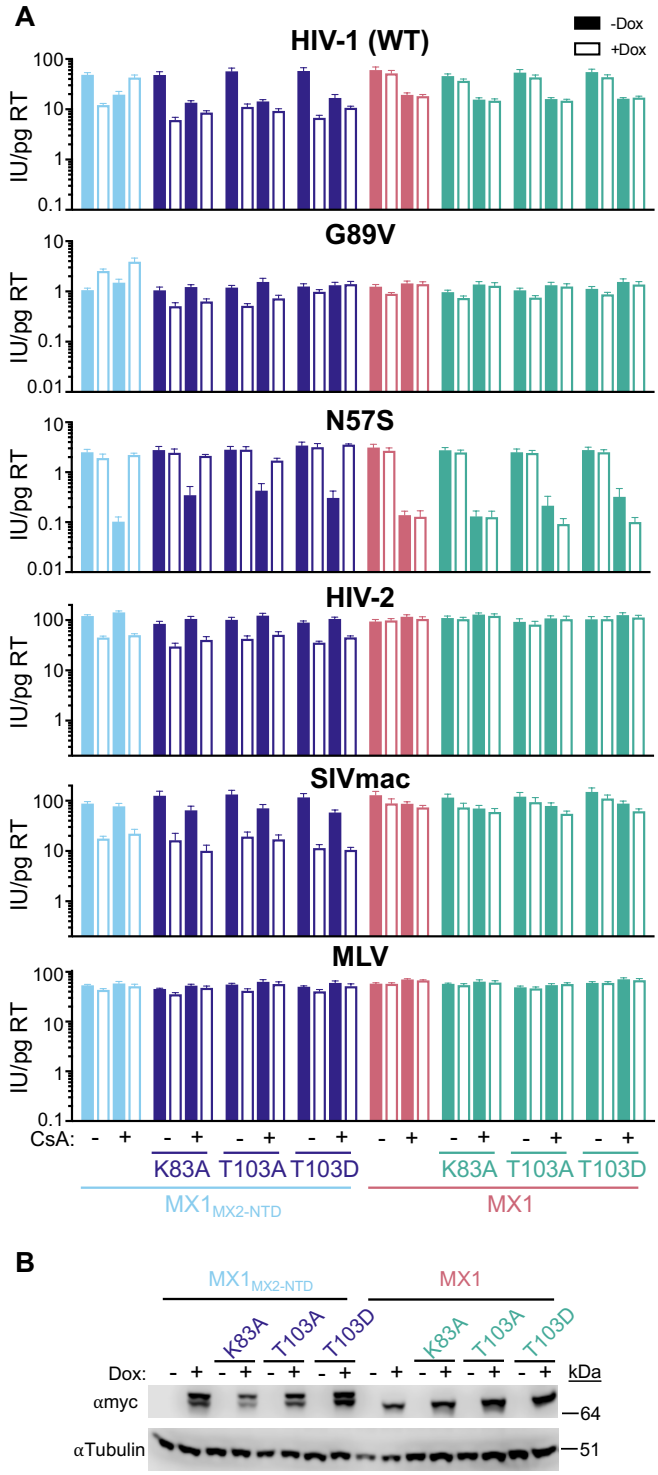

Figure 6. Antiviral activity of GTPase-deficient chimeric MX1$_{MX2\text{-}NTD}$ proteins.

A) Infection of HT1080 cells stably transduced with doxycycline-inducible myc-tagged MX1 or MX1$_{MX2\text{-}NTD}$ with the indicated mutations in the presence (open bars) or absence (filled bars) of doxycycline and presence or absence of CsA with the indicated GFP reporter viruses. Titers are represented as mean + sem of infectious units (IU) per pg of reverse transcriptase (RT), n≥9 technical replicates combined from three-seven independent experiments. Statistical analysis in S1 File.

B) Western blot analysis of doxycycline-inducible MX1$_{MX2\text{-}NTD}$ or MX1-myc and tubulin loading control.

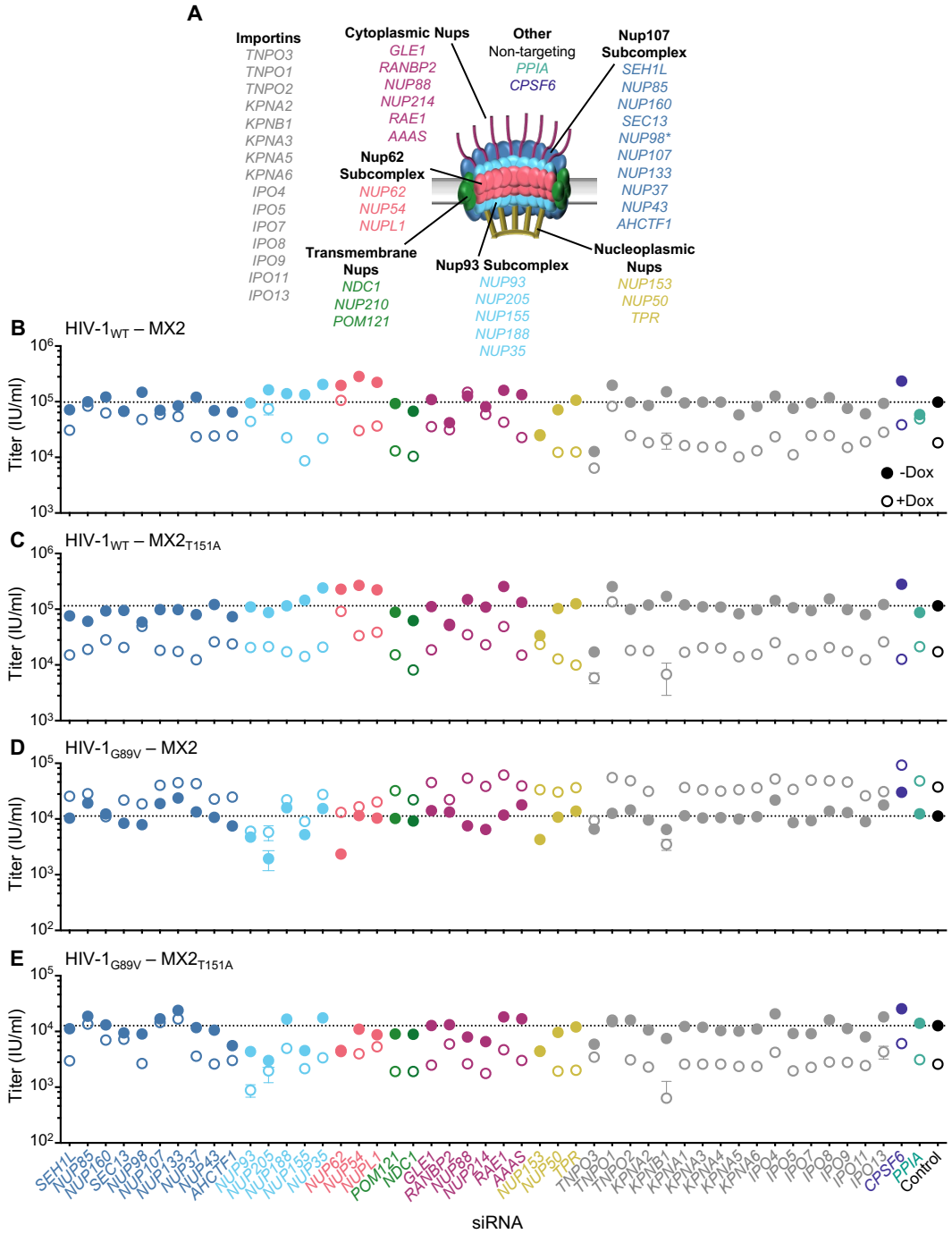

Figure 7. GTPase-deficient MX2 has distinct nucleoporin requirements for antiviral activity. A) Schematic representation of the nuclear pore complex and genes included in siRNA library color coded by subcomplex. (*- NUP98 is listed as a member of Nup107 subcomplex, however. Nup98 and Nup96 are produced following autoproteolytic cleavage of a polyprotein precursor (57, 58), this siRNA will target both Nups). Importins/nuclear transport receptors (NTRs) included in the siRNA library listed in grey. Also included, siRNA targeting CypA, CPSF6, and a non-targeting control siRNA.

B-D) Infectivity of HIV-1 GFP reporter viruses in HT1080 cells stably transduced with doxycycline-inducible MX2 or $MX2_{T151A}$ in the presence (open circles) or absence (filled circles) of doxycycline 64-72h after transfection with siRNA (color coded by subcomplex as in A). Titers are mean ± sem, n=3 technical replicates, representative of four independent experiments. Statistical analysis in S1 File.

759 **Supplementary Information legends**
760
761 **S1 Fig. Recognition of retroviral capsids by TRIMCyp fusions.**
762 A) Infectivity of GFP reporter viruses on HeLa cells stably expressing control empty vector, owl
763 monkey TRIMCyp (owmTRIMCyp), or chimeras of the TRIM5 N-terminal domain with human
764 cyclophilin A (huCypA), or human $CypA_{D66N}$, $CypA_{R69H}$, $CypA_{D66N/R69H}$ mutants. Titers are
765 represented as mean + sem of infectious units (IU) per mL, n=3 technical replicates representative
766 of five independent experiments. Statistical analysis in S1 File.
767 B) Expression of the TRIM fusion proteins tagged with HA and tubulin loading control in stable
768 cell lines used in (A).
769
770 **S2 Fig. Generation of CypA knockout and mutant cell lines.**
771 A) Schematic of the *PPIA* (CypA) locus on Chromosome 7 with crRNA guide targeting sites intron
772 1 and exon 4, and PCR primers for clone screening and verification indicated. Diagram of AAV
773 donor for homology-directed repair shown below, as well as amino acid residues 66-69 in wild-
774 type and mutant CypA cells.
775 B) Sequences of the wild-type locus at targeted sites, with crRNA and PAM sites indicated. Dots
776 indicate sequences flanking those shown in detail. Allele sequences of $CypA^{-/-}$ clones with
777 mismatches to wild-type sequence highlighted and deleted sequence indicated by dashes,
778 consequence of mutations in each knock-out allele shown below.
779 C) Sequences of wild-type and point-mutant alleles with nucleotide changes in codons and *Hpa*I
780 site in intron 3 indicated.
781 D) Top: Infectivity of HIV-1 GFP reporter virus infection in control, $CypA^{-/-}$ (left), and CypA-mutant
782 (right) cell clones expressing doxycycline-inducible MX2 in the presence (open bars) or absence
783 (filled bars) of doxycycline (Dox) and presence or absence of CsA. Alleles of CypA in knock-out
784 clones detailed in (B) are indicated. Titers are represented as mean + sem of infectious units (IU)
785 per pg of reverse transcriptase (RT); left: n≥6 technical replicates combined from three
786 independent experiments; right: n≥3 technical replicates representative of four independent
787 experiments. Statistical analysis in S1 File. Bottom: western blot analysis of doxycycline-inducible
788 MX2, CypA, and tubulin loading control in the indicated cell clones.
789
790 **S3 Fig. Validation of CA binding specificity by CypA mutants.**
791 HIV-1 WT, N57A, or G89V CA tubes were assembled *in vitro* and incubated with lysates from
792 control or CypA-mutant HT1080 cells as indicated. The reaction mixtures were subjected to
793 centrifugation to separated pulled-down (bound) fractions from unbound proteins in supernatants.
794 Lane 1: cellular lysates; Lane 2: supernatant from control experiments without CA tubes; Lanes
795 3-5: supernatants after incubating cellular lysates with CA tubes; Lane 6: pulled-down fraction
796 from control experiment in the absence of CA tubes; Lanes 7-10: proteins bound to CA tubes.
797
798 **S4 Fig. The effects of CsA on retroviral sensitivity to MX2 are the direct result of blocking**
799 **CA-CypA interactions.**
800 Infection of control or CypA-mutant HT1080 cells expressing doxycycline-inducible MX2 in the
801 presence (open bars) or absence (filled bars) of doxycycline (Dox) and present or absence of CsA
802 with indicated GFP reporter viruses. Titers are represented as mean + sem of infectious units (IU)
803 per pg of reverse transcriptase (RT), n≥6 technical replicates combined from two-three
804 independent experiments. Statistical analysis in S1 File.
805
806 **S5 Fig. Determinants for MX2 activity in the absence of CA-CypA interactions.**
807 A) Infectivity of GFP reporter viruses in HeLa cells expressing doxycycline-inducible C-terminally
808 myc-tagged MX2, MX2 mutants, or $MX1_{MX2\text{-}NTD}$ in the presence (open bars) and absence (filled
809 bars) of doxycycline (Dox). Cells were infected in the presence of CsA where indicated. Titers are
810 represented as mean + sem of infectious units (IU) per pg of reverse transcriptase (RT), n≥8
811 technical replicates combined from two-six independent experiments. Statistical analysis in S1
812 File.

B) Western blot analysis of doxycycline-inducible MX2-myc and tubulin loading control.

S6 Fig. Restriction of HIV-1 infection by GTPase-deficient MX2 in CypA mutant cells
A) Infection of control and CypA-mutant HT1080 cell clones stably transduced with doxycycline-inducible myc-tagged MX2 (left) or $MX2_{T151A}$ (right) in the presence (open bars) or absence (filled bars) of doxycycline and presence or absence of CsA with the indicated GFP reporter viruses. Titers are represented as mean + sem of infectious units (IU) per pg of reverse transcriptase (RT), n≥12 technical replicates combined from five independent experiments. Statistical analysis in S1 File.
B) Western blot analysis of doxycycline-inducible MX2-myc, CypA, and tubulin loading control in the indicated cell clones.

S7 Fig. Phosphorylation at residue T151 does not determine CypA-independent MX2 activity.
A) Infection HeLa cells stably transduced with doxycycline-inducible myc-tagged MX2 or $MX2_{T151D}$ in the presence (open bars) or absence (filled bars) of doxycycline and presence or absence of CsA with the indicated GFP reporter viruses. Titers are represented as mean + sem of infectious units (IU) per pg of reverse transcriptase (RT), n≥6 technical replicates combined from two-seven independent experiments. Statistical analysis in S1 File.
B) Western blot analysis of doxycycline-inducible MX2-myc and tubulin loading control.

S8 Fig. Restriction by GTPase-deficient MX2 in the absence of CA-CypA binding is not mediated by known CA-GTPase domain interactions.
A) Infection of HeLa cells stably transduced with doxycycline-inducible myc-tagged MX2 with or without mutations in the N-terminal triple-arginine motif ($_{11}AAA_{13}$), T151A, or CA-binding residues in the GTPase domain (SSE) in the presence (open bars) or absence (filled bars) of doxycycline and presence or absence of CsA with the indicated GFP reporter viruses. Titers are represented as mean + sem of infectious units (IU) per pg of reverse transcriptase (RT), n=9 technical replicates combined from three independent experiments. Statistical analysis in S1 File.
B) Western blot analysis of doxycycline-inducible MX2-myc and tubulin loading control.

S9 Fig. Antiviral activity of GTPase-deficient chimeric $MX1_{MX2\text{-}NTD}$ proteins.
A) Infection of HeLa cells stably transduced with doxycycline-inducible myc-tagged MX1 or $MX1_{MX2\text{-}NTD}$ with the indicated mutations in the presence (open bars) or absence (filled bars) of doxycycline and presence or absence of CsA with the indicated GFP reporter viruses. Titers are represented as mean + sem of infectious units (IU) per pg of reverse transcriptase (RT), n≥9 technical replicates combined from three-seven independent experiments. Statistical analysis in S1 File.
B) Western blot analysis of doxycycline-inducible $MX1_{MX2\text{-}NTD}$ or MX1-myc and tubulin loading control.

S10 Fig. Experimental design for Nup/NTR knockdown
A) Experimental strategy to investigate the roles of Nups and NTRs in antiviral activity of MX2 and $MX2_{T151A}$. For a detailed description, refer to the Materials and Methods.
B) Western blot analysis of doxycycline-inducible MX2 and $MX2_{T151A}$ and tubulin loading control.